

Multimodal Dataset Distillation for Image-Text Retrieval

Xindi Wu¹ Zhiwei Deng² Olga Russakovsky¹

¹Princeton University ²Google Research

princetonvisualai.github.io/multimodal_dataset_distillation

Abstract

Dataset distillation methods offer the promise of reducing a large-scale dataset down to a significantly smaller set of (potentially synthetic) training examples, which preserve sufficient information for training a new model from scratch. So far dataset distillation methods have been developed for image classification. However, with the rise in capabilities of vision-language models, and especially given the scale of datasets necessary to train these models, the time is ripe to expand dataset distillation methods beyond image classification. In this work, we take the first steps towards this goal by expanding on the idea of trajectory matching to create a distillation method for vision-language datasets. The key challenge is that vision-language datasets do not have a set of discrete classes. To overcome this, our proposed multimodal dataset distillation method jointly distill the images and their corresponding language descriptions in a contrastive formulation. Since there are no existing baselines, we compare our approach to three coreset selection methods (strategic subsampling of the training dataset), which we adapt to the vision-language setting. We demonstrate significant improvements on the challenging Flickr30K and COCO retrieval benchmark: the best coreset selection method which selects 1000 image-text pairs for training is able to achieve only 5.6% image-to-text retrieval accuracy (recall@1); in contrast, our dataset distillation approach almost doubles that with just 100 (an order of magnitude fewer) training pairs.

1 Introduction

Dataset distillation aims to create concise summaries of data that preserve most of the critical information of the original dataset. It can be used in place of the full dataset for model training and allows for more efficient Neural Architecture Search [1, 2], Continual Learning [3, 4, 5], Federated Learning [6, 7] and effective adaptation in resource-constrained settings (e.g., mobile platforms, robotic platforms) [8, 9]. There has been a growth of dataset distillation methods developed for image classification datasets (e.g., [10, 11, 12, 13, 14, 15, 16, 17, 18, 19, 20, 21, 22, 23, 24, 25, 26, 27]), where the goal is to capture sufficient information for each class to be able to accurately reconstruct the discriminative boundaries. However, considering the recent progress in multimodal machine learning, particularly the development of large foundation models [28, 29] such as CLIP [30], BERT [31], UNITER [32], FIAVA [33], BLIP [34, 35], Gato [36], Flamingo [37], PALM [38], it is worth noting that all of these models require massive-scale datasets. In the context of vision-language tasks, the importance of dataset distillation is twofold. Firstly, it enables the development of more efficient and resource-friendly training that can effectively handle the complexities of vision-language datasets. Secondly, it facilitates the learning of correspondence between visual and textual elements, which is crucial for various vision-language tasks.

Goal. In this work, we create the first distillation method for vision-language datasets. Concretely, given a dataset consisting of a set of images with corresponding language descriptions, our method creates a set of synthetic images and corresponding text embeddings which can be used to train a

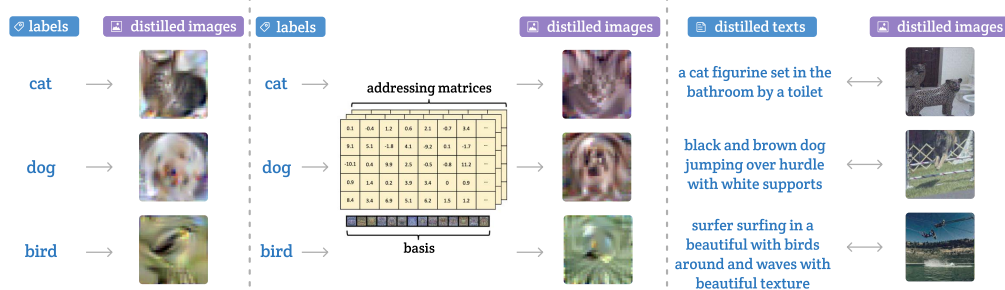


Figure 1: **Dataset Distillation Comparison.** (Left) Prior dataset distillation methods [10, 12, 18] are class-specific; i.e., they distill the key information for each individual discrete class. (Center) Even the recently-developed method of [24] which enables information sharing between classes through learned bases still assumes a discrete set of classes. (Right) In contrast, we set out to distill vision-language datasets with no discrete classes; we do so via a novel method which jointly distills the vision and text.

model to learn the correspondence between a new image and a text description. We evaluate this model on image-to-text and text-to-image retrieval tasks.

Challenges. The first key challenge, and the main difference from prior dataset distillation work [10, 12, 24] is that vision-language datasets do not contain a discrete set of classes to ground the distillation process. Instead, these datasets contain intricate cross-modal relationships and nuances between the visual and textual elements, requiring a co-distillation approach. The second challenge, which derives from these complex cross-modal relationships, is the computational complexity. Prior dataset distillation methods were developed on small-resolution (typically 28x28 or 32x32 images, as in MNIST [39] or CIFAR [40]), and nevertheless suffer from significant computational costs when creating the distilled dataset. In contrast, vision-language datasets contain higher-resolution images, and models trained on these dataset are significantly more complex. Thus, developing a practical method for distilling vision-language dataset requires grappling with the associated computational challenges.

Contributions. To the best of our knowledge, this work is the first to tackle multimodal dataset distillation. In doing so, we make the following key contributions.

1. We highlight the challenges of vision-language dataset distillation and establish the first set of baselines for this task by adapting three coresets selection methods [41, 42, 43, 44].
2. We propose a method that jointly performs vision-language co-distillation. Our method is not restricted to discrete classes, in contrast to prior image classification dataset distillation methods, and is computationally tractable to operate on the high-resolution images and complex backbone networks.
3. Our method significantly improves image-to-text and text-to-image retrieval on the challenging Flickr30K [45] and COCO [46] dataset, outperforming models trained with coreset selection methods at the same scale. For example, we demonstrate that the best coreset selection method (K-center [43, 44]) achieves 5.6% image-to-text retrieval accuracy (recall@1, retrieving from 126 options) after selecting 1000 image-text pairs for training. In contrast, our method almost doubles that performance on the same task with **an order of magnitude** fewer (just 100) distilled image-text pairs. Similarly, K-center can achieve up to 3.2% text-to-image retrieval accuracy with 1000 pairs, while our method achieves 9.1 ± 0.5 % with the full 1000 pairs and 4.7 ± 0.2 % with just 100 pairs.

As we continue to see an explosion in multimodal datasets, it becomes even more crucial to develop mechanisms that can efficiently and effectively distill insights from these multifaceted sources. We hope this work jump-starts further research into this important and challenging space of multimodal dataset distillation.

2 Related Works

Dataset Distillation. The concept of dataset distillation, first introduced in [10], demonstrated that a handful of synthetic images can achieve comparable performance to that of the original MNIST dataset. Meta-learning based data distillation approaches [10, 19, 24, 47] typically use bilevel optimization, where the inner loop trains on the distilled data samples and the outer loop optimizes the meta dataset. They take gradients with respect to the learned data samples and a few recent works [17, 18, 20, 47] focus on addressing the significant amount of meta-gradient computation challenges. [18] proposed a kernel-inducing points meta-learning algorithm and leverage the connection between infinitely wide convnet and kernel ridge regression. To avoid unrolling recursive computation graph and provide denser supervision on distilled data, [48] proposed an approximate optimization of matching gradients w.r.t. real and distilled training data, yet it still involves bilevel optimization and second-order derivatives.

Several works [12, 13, 14, 48, 49, 50] explored gradient or trajectory matching methods for dataset distillation, and those approaches focus on matching the gradient or trajectory of the gradient w.r.t. the model trained on the real and distilled data. Our work is mostly inspired by the trajectory matching method [12], which is more efficient for optimization since they mostly do not involve long unrolling computation graph. Rather than aligning model gradients, another thread of work [15, 49, 50] are developed to align feature distributions between real and distilled data using distribution divergence metric in the latent space. While most prior approaches only target at vision datasets, a few studies have also investigated dataset distillation for language, [27] simultaneously distills images and soft labels, and [51] learns soft labels without synthetic images. [52] distills critical text classification data, and TESLA [53] scales to ImageNet-1K with image per class equals to 10 and 50. Our work is the first to scale up dataset distillation methods to multimodal tasks, which involves creating distilled data that capture critical features and complex relationships within and between two modalities.

Multimodal Distillation. Prior works on multimodal distillation primarily centered on knowledge distillation. [54] proposed distilling knowledge from a pre-trained teacher model into an image encoder, focusing on recognizing visual concepts that align with objects and attributes in captions. The multi-teacher alignment method from [55] enables self-supervised knowledge distillation from multimodal teacher networks to guide the student network training. It is worth noting that while both [54] and [55] explore multimodal distillation, their focus is primarily on knowledge distillation. It transfers knowledge from a larger teacher model to a smaller student model to improve the latter’s performance. In contrast, our study focuses on multimodal dataset distillation and is fundamentally a data-centric pragmatic compression problem. The goal is to find equivalent bits that can represent the entire multimodal datasets.

Cross-modal Retrieval. Most cross-modal retrieval methods function at the representation level, and it encourages a joint embedding space by measuring the similarities between learned representations across different modalities [56, 57], allowing for the retrieval of queries and data across these different modalities [58, 59, 60, 61, 62, 63]. For image-text retrieval, it focuses on the retrieval of images given captions, or of captions for a query image [64, 65, 66, 67]. Many techniques are developed to produce representations that are semantically similar for image-text pairs [68, 69, 70, 71]. [72] incorporates hard negatives in their loss function, [73, 74] seeks to measure the fine-grained similarity for cross-modal matching, and [60] proposed noisy correspondence rectifier for robust cross-modal retrieval. More advanced image-text alignment methods [33, 34, 37, 75, 76] usually combined with pretraining have been developed recently and showed promising results on image-text retrieval tasks. [32] introduced an optimal-transport based word-region alignment pretraining method. [77] diagnose language bias in recent vision-language datasets and proposed a debias method for retrieval tasks. [78] proposed iterative matching method with recurrent attention memory. In this work, we evaluate our multimodal dataset distillation method on image-text retrieval tasks.

3 Method

We propose a multimodal dataset distillation method for distilling a large-scale image-text dataset into a smaller, information-rich dataset, that maintains the relevance for training models associated with the original dataset. The detailed method is illustrated in Fig. 2.

3.1 Problem Formulation

Consider a large-scale dataset $\mathbf{D} = \{(x_i, y_i)\}_{i=1}^N$, where each x_i denotes an image and each y_i denotes their corresponding text descriptions; note that in practice, y_i is a set $\{y_{i1}, y_{i2}, \dots, y_{iK}\}$ where K is the number of descriptions associated with each image. Our goal is to learn a smaller dataset $\hat{\mathbf{D}} = \{(\hat{x}_j, \hat{y}_j)\}_{j=1}^M$, with significantly fewer data pairs $M \ll N$ that still captures most of the essential information needed to train a vision-language model effectively.

Concretely, consider a vision-language model f for image-text retrieval, with parameters θ (consisting of θ_{img} and θ_{txt} corresponding to the image and text inputs respectively). This model can be trained by optimizing the similarity loss which encourages alignment between the image and text embeddings:

$$\theta^* \approx \arg \min_{\theta} \frac{1}{N} \sum_{i=1}^N \ell(f(x_i; \theta_{img}), f(y_i; \theta_{txt})), \quad (1)$$

either on the full dataset \mathbf{D} , or on the smaller dataset $\hat{\mathbf{D}}$, yielding the parameters $\hat{\theta}$. Eqn. 1 ensures that the model correctly learns to match the two modalities.

Our goal is to distill a dataset $\hat{\mathbf{D}}$ such that parameters θ^* and $\hat{\theta}$ obtain comparable vision-language matching performance. More specifically, consider a metric \mathbf{m} defined to quantify the correlation between the model’s representation $f(x; \theta_{img})$ of a given image x and the representation $f(y; \theta_{img})$ of a given text y , this representation should match the actual similarity between the image and text pair. The calculation of this correlation is based on whether the image and text pair is a positive (matching) or a negative (non-matching) pair. Given the test dataset \mathbf{D}_{te} , our objective can be defined as follows. Importantly, even when the model is trained on the distilled dataset $\hat{\mathbf{D}}$, we still evaluate its performance on the original test dataset \mathbf{D}_{te} to ensure a fair measurement of our method.

$$\mathbb{E}_{(x,y) \sim \mathbf{D}_{te}} [\mathbf{m}(f(x; \theta_{img}^*), f(y; \theta_{txt}^*))] \simeq \mathbb{E}_{(x,y) \sim \mathbf{D}_{te}} [\mathbf{m}(f(x; \hat{\theta}_{img}), f(y; \hat{\theta}_{txt}))], \quad (2)$$

when creating the dataset $\hat{\mathbf{D}}$, the pairs (\hat{x}, \hat{y}) can be subsampled from the original set \mathbf{D} , as described by the coreset selection methods elaborated below in Section 3.2. However, a more effective strategy is to learn *synthetic* image-text pairs (\hat{x}, \hat{y}) which can be more descriptive. In Section 3.3 we introduce our multimodal dataset distillation method.

Connection with Standard Dataset Distillation. Traditionally, dataset distillation is tailored for classification tasks with discrete labels, where each label possesses its distinctive set of distilled data. These distilled datasets are compact and enable efficient learning while preserving important information. We take this concept a step further in the multimodal scenario, where we distill information from both vision and language data. This involves creating synthetic data that capture critical features and relationships within and between these two modalities. As opposed to merely classifying discrete labels, we are looking at a more complex, interconnected dataset where the relation between vision and language data is crucial. Our method considers the correlation between image and text data and how they influence each other. It is worth noting that this would be impossible if we solely optimize a single modality, which is supported by our single-modality distillation results in Table 4 and will be discussed later in Sec 4.2.

3.2 Baselines: Coreset Selection

Since, to the best of our knowledge, there is no pre-existing work in the domain of multimodal dataset distillation, we begin by formulating a set of baselines to construct the smaller dataset $\hat{\mathbf{D}}$. These baselines are based on coreset selection methods, where a subset of the training pairs (x_i, y_i) is chosen, up to a given budget of M pairs, as to maximize the “informativeness” of the selected subset. We consider three such methods, adapted from prior work.

Herding [41]. The core idea of herding is to greedily select a set of pairs for $\hat{\mathbf{D}}$ that are as similar as possible from other pairs already selected. To do so, we use pre-trained image and text encoders, respectively, to extract feature representations of the image x_i text y_i pairs and then concatenate the features, and calculate the “center” of the dataset in this feature space. This is done by simply averaging the feature vectors for all image-text pairs in the dataset. We use the Euclidean distance as a

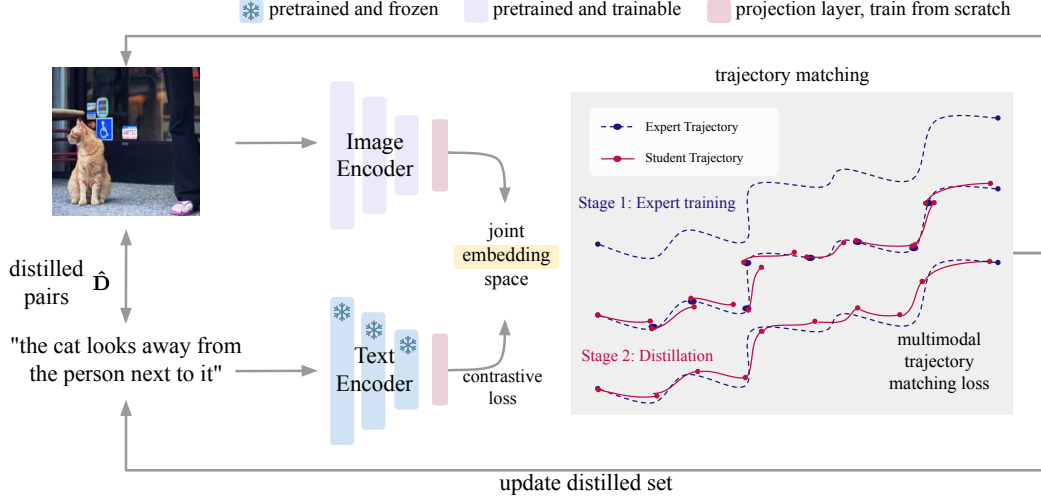


Figure 2: **Multimodal Dataset Distillation.** $\hat{\mathbf{D}}$ represents the distilled vision-language dataset. Both the image and text encoders are pretrained and the text encoder is frozen. They are both followed by a trainable projection layer. The contrastive loss is used to measure the distance between the paired image-text embeddings, which in turn influences the trajectory updates during distillation. On the right panel, we show how training with distilled data aligns its trajectory to the expert’s, from randomly selected starting point on the expert trajectory. The distilled dataset is updated based on multimodal trajectory matching loss between the student and expert parameter trajectories.

distance metric in the feature space. We start with an empty coreset and then for each iteration, add the image-text pair from the dataset that is closest to the current “center” of the coreset to minimize the distance between the coreset center and dataset center. After adding a new data point, we recalculate the center of the coreset based on the data points currently in it.

K-center [43, 44]. This baseline is similar to herding except it selects the training examples to be as far apart as possible from each other, without summarizing the selection by computing a single center. Concretely, we concatenate the features of the image and text pairs and start by randomly selecting a single data point. Then, for each iteration, until finishing selecting K points, we add a new image-text pair from the dataset that is *furthest* in Euclidean distance from the nearest example already selected. The drawback of this method is its high computational cost, especially with large datasets, as it involves heavy distance calculations between data points every iteration.

Forgetting [42]. The core idea of the third baseline is to directly identify training examples that are learned the most *reliably* by the original model trained on the full dataset. Concretely, during each training epoch, we assess the correctness of the model’s prediction for every image-text pair in the context of the specific task (i.e., image-text retrieval). A forgetting event is registered for an image-text pair when the model correctly predicts the example in one epoch but fails in the next. We continually track these forgetting events for each pair during training, to identify those image-text pairs that have experienced the *fewest* forgetting events. The coreset is formed by selecting either a fixed number of top pairs, or all pairs below a certain forgetting event threshold.

3.3 Trajectory-Guided Multimodal Dataset Co-Distillation

The coreset selection methods described above, while effective to some extent, demonstrate certain limitation as they only rely on selecting a subset of the training dataset \mathbf{D} . This restriction leads to less effective results compared to our dataset distillation method, as it provides the flexibility to generate an optimized distilled dataset $\hat{\mathbf{D}}$, and the learning process efficiently helps extract the most essential information embedded in \mathbf{D} . Not only does this lead to decreased storage and computational requirements, but it also optimizes the performance of the model trained on this distilled dataset.

Here we describe our multimodal dataset distillation framework, building off of the idea of matching training trajectories (MTT) [12] developed for distilling image classification datasets. The core idea

of trajectory matching is that the dataset distillation can be achieved by implicitly matching the by-product, which is the parameter trajectory of the distilled dataset and the original full dataset, given direct information extraction is not feasible. Concretely, we can compute a loss function on the cumulative discrepancy between the expert parameter trajectory θ^* obtained from training a model on the full dataset \mathbf{D} and the parameters $\hat{\theta}$ obtained from training a model on the distilled dataset $\hat{\mathbf{D}}$, and use that loss to guide the creation of a better $\hat{\mathbf{D}}$, one that can match the parameters θ^* more closely.

The approach consists of two stages:

1. Obtaining the expert training trajectories $\{\tau^*\}$, with each trajectory $\tau^* = \{\theta_t^*\}_{t=0}^T$, by training multiple models for T epochs on the full dataset \mathbf{D} . For our multimodal setting, the models are trained using **bidirectional contrastive loss**, described below.
2. Training a set of student models on the current distilled dataset $\hat{\mathbf{D}}$ using the same bidirectional contrastive loss, and then updating the distilled dataset $\hat{\mathbf{D}}$ based on the **multimodal trajectory matching loss** of the student models' parameters and the optimal θ^* .

Bidirectional Contrastive Loss. We train both the expert and the student vision-language models using the bidirectional contrastive loss, following the formalism of [30] as it is effective for learning shared image-text representation. Concretely, given a batch of n image-text pairs $\{(x, y)\}$, either from the real dataset \mathbf{D} or from the synthetic distilled dataset $\hat{\mathbf{D}}$, we jointly learn the encoders $f(x; \theta_{img})$ and $f(y; \theta_{txt})$ such that the cosine similarity of all correct image-text pairs is high and that of the incorrect pairs ($n^2 - n$) is low. Cosine similarity is defined as:

$$\alpha(x, y) = \frac{\langle f(x; \theta_{img}), f(y; \theta_{txt}) \rangle}{\|f(x; \theta_{img})\| \|f(y; \theta_{txt})\|}. \quad (3)$$

We then compute bidirectional contrastive losses composed of an image-to-text matching loss and a text-to-image matching loss, following the form of the InfoNCE loss [79]:

$$\ell_{contrastive} = -\frac{1}{2n} \sum_{(x, y) \text{ in batch}} \left(\log \frac{\exp(\alpha(x, y))}{\sum_{y'} \exp(\alpha(x, y'))} + \log \frac{\exp(\alpha(x, y))}{\sum_{x'} \exp(\alpha(x', y))} \right). \quad (4)$$

To imitate the effect of training data on parameter trajectories, we use the same objective function to guide the update of parameters $\theta_{img}, \theta_{txt}$ during both expert training (stage 1) and distillation (stage 2). Notably, while hard negative mining is typically used in conjunction with contrastive loss, here we rely fully on the dataset distillation process itself without additional intervention. This process inherently considers hard negatives, it distills samples that are hard negative samples for others, which are eventually effective samples for learning. Dataset distillation can potentially by-pass the traditional hard negative mining complexities through the learning process.

Multimodal Trajectory Matching Loss. Following the MTT [12] formulation, we randomly sample M image-text pairs from \mathbf{D} to initialize the distilled dataset $\hat{\mathbf{D}}$ (more details can be found in the Sec 4.1). We sample an expert trajectory (i.e., the trajectory of a model trained on the full dataset) $\tau^* = \{\theta_t^*\}_{t=0}^T$ and a random starting epoch s to initialize $\hat{\theta}_s = \theta_s^*$. We train the student model on the distilled dataset for \hat{R} steps to obtain $\hat{\theta}_{s+\hat{R}}$. We then update the distilled dataset based on multimodal trajectory matching loss $\ell_{trajectory}$ computed on the accumulated difference between student trajectory and expert trajectory:

$$\ell_{trajectory} = \frac{\|\hat{\theta}_{img, s+\hat{R}} - \theta_{img, s+R}^*\|_2^2}{\|\theta_{img, s}^* - \theta_{img, s+R}^*\|_2^2} + \frac{\|\hat{\theta}_{txt, s+\hat{R}} - \theta_{txt, s+R}^*\|_2^2}{\|\theta_{txt, s}^* - \theta_{txt, s+R}^*\|_2^2}. \quad (5)$$

We update the distilled dataset by back-propagating through multiple (\hat{R}) gradient descent updates to the $\hat{\mathbf{D}}$, specifically, image pixel space and text embedding space with respect to Eqn. 5. We initialize the continuous sentence embeddings using a pretrained BERT model and update the distilled text in the continuous embedding space. For the distilled image optimization, we directly update the pixel values of the distilled images. The full details are described in Algorithm 1.

4 Experiments

We first describe the cross-modal retrieval test-bed in Sec. 4.1. We use it to evaluate our multimodal dataset co-distillation performance. We then compare our method to other baseline approaches and

Algorithm 1 multimodal dataset co-distillation

Require:

- $(\tau_{img}^*, \tau_{txt}^*)$: a set of expert parameter trajectories, each of length T epochs, trained on the full dataset \mathbf{D}
 M : target size of distilled dataset
 T^+ : maximum start epoch
 R : number of updates between starting and target expert parameters
 \hat{R} : number of updates to student network per distillation step
 α_0 : initial learning rate.
- 1: Initialize distilled data $\hat{\mathbf{D}} \sim \mathbf{D}$
 - 2: Initialize trainable learning rate $\alpha := \alpha_0$ for training student models on $\hat{\mathbf{D}}$
 - 3: **for each** distillation step **do**
 - 4: ▷ Randomly sample an expert trajectory $(\tau_{img}^*, \tau_{txt}^*)$, corresponding to $\{(\theta_{img,t}^*, \theta_{txt,t}^*)\}_{t=0}^T$
 - 5: ▷ Choose random start epoch, $s \leq T^+$
 - 6: ▷ Initialize the student network with expert params $\hat{\theta}_{img,s} := \theta_{img,s}^*$ and $\hat{\theta}_{txt,s} := \theta_{txt,s}^*$
 - 7: **for** \hat{R} iterations **do**
 - 8: ▷ Sample a mini-batch of distilled dataset $\hat{\mathbf{D}}$
 - 9: ▷ Use the contrastive loss of Eqn. 4 to update the parameters $\hat{\theta}_{img}$ and $\hat{\theta}_{txt}$
 - 10: **end for**
 - 11: ▷ Compute loss $\ell_{trajectory}$ between expert params $\theta_s^*, \theta_{s+R}^*$ and distillation params $\hat{\theta}_{s+\hat{R}}$ using Eqn. 5
 - 12: ▷ Update distilled dataset $\hat{\mathbf{D}}$ and learning rate α with respect to $\ell_{trajectory}$
 - 13: **end for**
 - 14: **Output:** Distilled data $\hat{\mathbf{D}}$ and learning rate α .
-

conduct a set of ablation studies to understand the impact of unimodal (image-only and text-only) distillation in Sec. 4.2.

4.1 Evaluation Test-Bed

Datasets and Tasks. We evaluate our method on standard vision-language datasets: Flickr30K [45] and COCO [46], which are widely used in prior image-text retrieval studies. We use them for both stage 1 expert training and stage 2 distillation. We use the Karpathy split [80], Flickr30K has splits of 29k/1k/1k images and COCO 113/5k/5k images for train/validation/test. Each image is paired with five captions. We conducted both image-to-text retrieval (TR) and text-to-image retrieval (IR). Given a query from one modality, the aim is to retrieve the closest matches from the other modality using cosine distance for measuring feature similarity. We use R@K (for $K \in \{1, 5, 10\}$) as evaluation metric to compute the fraction of times the correct result appears among the top K items.

Network Architectures. We primarily use ImageNet [81, 82] pretrained, trainable NormalizerFree ResNet (NFNet) [83] (specifically, NFNet_I0 [83] from timm library [84]) as the image encoder following Flamingo [37]. The text embedding branch is a BooksCorpus [85] and English Wikipedia pretrained and frozen BERT [31]. Each encoder is followed by a trainable linear projection layer using Kaiming uniform initialization [86]. Using a trainable BERT adds additional complexity which is orthogonal to multimodal dataset distillation and we believe it is out of scope of this work. While both the encoders are pretrained, they are only pretrained on unimodal data with no exposure to the other modality. These two pretrained models serve as a common foundation and good starting point. See Appendix Sec. 7.3 for more discussions. We also provided ablation studies in the Appendix Sec. 7.2 to experiment with different vision/language backbones. The network is unrolled over a fixed number of synthetic steps, which matches the accumulated gradients of the updated trajectory over distilled dataset to the expert trajectory over several steps. We observed that the larger synthetic steps often result in improved performance, see Appendix Sec. 7.4 for more details.

Implementation. Our models are implemented in PyTorch [87], for the expert training stage, we train on a single RTX 3090 GPU with 24GB for 10 epochs, where a single epoch takes 40 minutes of wall-clock time. We save 20 image-text paired expert trajectories in the model pool. The purpose of sampling from a diverse set of parameter trajectories for distillation is to encourage the distilled

dataset to incorporate diverse information, and this helps in better generalization and avoids overfitting to a particular step. We followed the data augmentation techniques used in [34], including resizing, cropping, flipping, and `RandomAugment` from `transform.randaugment` package. For the distillation stage, we train on one 8-GPU A6000 node. It takes 7 - 15 GPU hours depending on the setting (i.e. learning rate, distilled dataset size, etc.). For the final distilled text visualization, we find the nearest neighbours of the distilled text embeddings in the original training set embedding space, specifically, we compute the cosine similarity with all pre-computed training set sentence embeddings to determine the closest one. We use a trainable learning rate α to update the student network, which is initially set to 0.1. We use SGD with momentum=0.5, the learning rate for updating α , distilled image pixels and distilled text embeddings are 1e-02, 500 and 1000, respectively.

Initialization. We follow the same practice as in previous studies [12, 18, 47, 48] and initialize the distilled dataset with randomly selected pairs of real samples. We randomly select $n \in \{100, 200, 500, 1000\}$ image-text pairs from the original dataset for co-distillation. Specifically, the images have 224×224 resolution, and for the captions, we use their 768-dimensional sentence embeddings obtained from the pretrained BERT model. Our findings in Tab. 5 in the Appendix Sec. 7.1 show that initializing images from Gaussian distribution results in significantly lower performance. The complexity of images makes learning from random initializations challenging. In contrast, there is little difference in performance between using real and randomly initialized text embeddings. This shows that our co-distillation process encourages the language branch to transform ‘noise’ text embeddings into meaningful sentences that pair with the corresponding images. Surprisingly, despite the initial lack of semantic meaning between ‘noise’ texts and real images, we found notable semantic similarity between distilled text and real images, suggesting potential applications of our method in Visual Question Answering (VQA).

4.2 Model Analysis

Quantitative Results. As shown in Table 1, we observe that although there is relatively little variation in performance across each of the coreset selection baselines which we compare to, dataset distillation outperforms the best alternative by anywhere between 71% and 684%, with the relative improvement increasing when fewer pairs are used for training and for smaller values of K in $R@K$. Moreover, we note that with 1000 pairs, almost 30 times fewer examples than in the original dataset, our data distillation approach reaches 45.7% $R@10$ for text retrieval, relative to a practical upper bound of 75.2% from training on the entire dataset, and 33.48% for image retrieval $R@10$, relative to an upper bound of 69.7%. We also observe that the performance among the baseline coreset selection methods varies only slightly, with no single method consistently outperforming the others across all pair sizes and retrieval metrics, often matching or underperforming random selection. This suggests limitations to these coreset selection methods in multimodal settings. We report the practical upper/lower performance limits in Table 3. Note that the upper bound results here do not reflect the SOTA performance, but a full dataset training under the same training setting. We also keep the BERT backbone frozen for a fair comparison.

Qualitative Results. Here we provide a set of visualizations that depict the evolution of synthetic images changing over time in Fig. 3. Please see the Appendix for more details on the changes of textual content across different iterations of the distillation process.

Ablation. We conduct ablation studies to compare co-distillation to distillation where we keep one of the input modalities fixed. Results are in Table 4, which shows the image-text retrieval performance of three different approaches: text-only distillation, image-only distillation, and co-distillation. For all tasks and metrics the joint co-distillation method clearly outperforms the text-only and image-only distillation. For example, with 1000 training pairs in the distilled dataset, when performing image-to-text retrieval (TR), the text-only distillation achieves 7.7% top-1 recall, image-only distillation achieves slightly lower at 5.0%, and co-distillation beats both at 13.2%.

We observed that the improvement of text-only distillation was generally less than that of image-only distillation, with a few key caveats. First, image retrieval performance with a thousand training pairs is essentially independent from the distilled single modality. On the other hand, with a thousand training pairs text retrieval performance is still substantially better for the text-only distillation. In contrast, image-only distillation outperforms text-only distillation almost everywhere else. This may not be surprising: a good description of an image typically contains only a salient but small portion of the information present in an image. On the other hand, descriptions in our evaluated datasets

#pairs	Ratio%	Retrieval Metrics		Coreset Selection				Distillation (ours)
				Random	Herding	K-center	Forgetting	
100	0.34	TR	R@1	1.3	1.1	0.6	1.2	9.9 ± 0.3
			R@5	5.9	4.7	5.0	4.2	28.3 ± 0.5
			R@10	10.1	7.9	7.6	9.7	39.1 ± 0.7
		IR	R@1	1.0	0.7	0.7	0.7	4.7 ± 0.2
			R@5	4.0	2.8	3.1	2.4	15.7 ± 0.5
			R@10	6.5	5.3	6.1	5.6	24.6 ± 1.0
200	0.68	TR	R@1	2.1	2.3	2.2	1.5	10.2 ± 0.8
			R@5	8.7	8.4	8.2	8.4	28.7 ± 1.0
			R@10	13.2	14.4	13.5	10.2	41.9 ± 1.9
		IR	R@1	1.1	1.5	1.5	1.2	4.6 ± 0.9
			R@5	4.8	5.5	5.4	3.1	16.0 ± 1.6
			R@10	9.2	9.3	9.9	8.4	25.5 ± 2.6
500	1.67	TR	R@1	5.2	5.1	4.9	3.6	13.3 ± 0.6
			R@5	18.3	16.4	16.4	12.3	32.8 ± 1.8
			R@10	25.7	24.3	23.3	19.3	46.8 ± 0.8
		IR	R@1	2.4	3.0	3.5	1.8	6.6 ± 0.3
			R@5	10.5	10	10.4	9.0	20.2 ± 1.2
			R@10	17.4	17.0	17.3	15.9	30.0 ± 2.1
1000	3.45	TR	R@1	5.2	5	5.6	3.1	13.3 ± 1.0
			R@5	15.6	14.6	16.1	14.9	34.8 ± 1.2
			R@10	22.5	22.2	24.1	20.9	45.7 ± 1.7
		IR	R@1	3.3	3.2	3.2	2.9	9.1 ± 0.5
			R@5	10.6	10.6	11.3	9.2	24.1 ± 1.0
			R@10	17.0	16.9	17.4	15.9	33.8 ± 2.0

Table 1: **Baseline comparisons on Flickr30K.** We compare our distillation method to four coreset selection methods: random selection of training examples, Herding [41], K-center [43, 44] and Forgetting [42]. We consider different selected sizes (100, 200, 500, and 1000) and report the image-to-text (TR) and text-to-image (IR) retrieval performance on the Flickr30K dataset. Ratio (%): the ratio (in percent) of the distilled set to the entire training set. We report our distillation results along with standard deviation, they are calculated from the performance of five differently initialized models after training on the same distilled dataset.

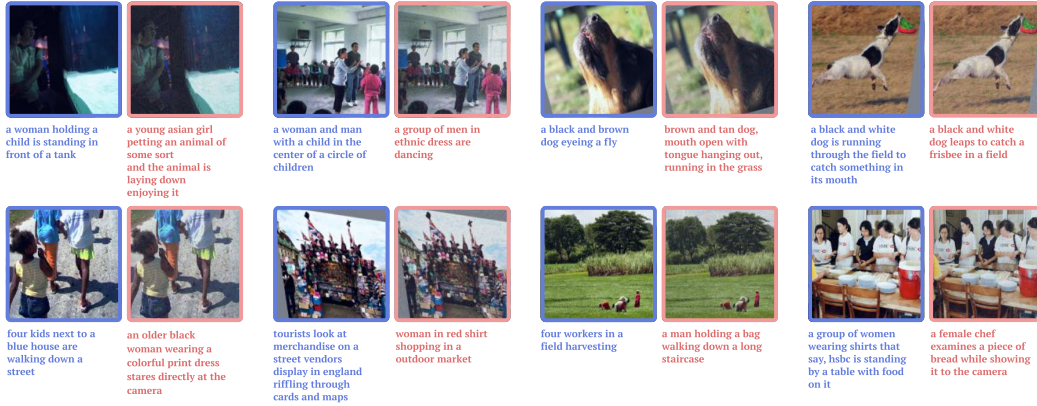


Figure 3: **Before and After Distillation.** (Left) The image and text pairs before the distillation. (Right) The image and text pairs after 2000 distillation steps. Note that the texts visualized here are nearest sentence decodings in the training set corresponding to the distilled text embeddings.

typically contain no information that cannot be inferred from the images. By modifying the images to text-relevant aspects, the optimization can highlight essential image features, but modifying text features can only introduce more information. Thus, if we interpret each original image as having substantially more information than its original sentence, we would expect image-only distillation to

#pairs	Ratio %	Retrieval Metrics	Coreset Selection				Distillation	
			Random	Herding	K-center	Forgetting	(ours)	
100	0.08%	TR	R@1	0.8	0.8	1.4	0.7	2.5 ± 0.3
			R@5	3.0	2.1	3.7	2.6	10.0 ± 0.5
			R@10	5.0	4.9	5.5	4.8	15.7 ± 0.4
		IR	R@1	0.3	0.5	0.4	0.3	1.3 ± 0.07
			R@5	1.3	1.4	1.4	1.5	5.4 ± 0.3
			R@10	2.7	3.5	2.5	2.5	9.5 ± 0.5
200	0.17%	TR	R@1	1	1.0	1.2	1.1	3.3 ± 0.2
			R@5	4.0	3.6	3.8	3.5	11.9 ± 0.6
			R@10	7.2	7.7	7.5	7.0	19.4 ± 1.2
		IR	R@1	0.6	0.9	0.7	0.6	1.7 ± 0.05
			R@5	2.3	2.4	2.1	2.8	6.5 ± 0.4
			R@10	4.4	4.1	5.8	4.9	12.3 ± 0.8
500	0.44%	TR	R@1	1.9	1.9	2.5	2.1	5.0 ± 0.4
			R@5	7.5	7.8	8.7	8.2	17.2 ± 1.3
			R@10	12.5	13.7	14.3	13.0	26.0 ± 1.9
		IR	R@1	1.1	1.7	1.1	0.8	2.5 ± 0.5
			R@5	5.0	5.3	6.3	5.8	8.9 ± 0.7
			R@10	8.7	9.9	10.5	8.2	15.8 ± 1.5
1000	0.88%	TR	R@1	1.9	2.4	2.4	1.9	6.8 ± 0.4
			R@5	7.6	9.0	9.0	7.7	21.9 ± 1.2
			R@10	12.74	13.98	14.11	13.02	31.0 ± 1.5
		IR	R@1	1.5	1.3	1.5	0.7	3.3 ± 0.1
			R@5	5.6	5.7	7.1	4.6	11.9 ± 0.5
			R@10	9.6	10.1	10.9	8.0	22.1 ± 0.9

Table 2: **Baseline comparisons on COCO.** Following the experiment setting for Flickr30K, we also compared our method to the coreset selection methods. Given the larger size of COCO relative to Flickr30K, the same number of pair settings results in a significantly smaller ratio of the full training set.

Dataset	Lower Bound: Random Ranking [88]						Upper Bound: Full Dataset					
	TR			IR			TR			IR		
	R@1	R@5	R@10	R@1	R@5	R@10	R@1	R@5	R@10	R@1	R@5	R@10
Flickr30K	0.1	0.6	1.1	0.1	0.5	1.0	33.9	65.1	75.2	27.3	57.1	69.7
COCO	0.02	0.1	0.2	0.02	0.1	0.2	19.6	45.6	59.5	16.9	41.9	55.9

Table 3: **Practical Limits Comparison.** A side-by-side comparison of the image-to-text (TR) and text-to-image (IR) retrieval results obtained from (*lower bound, left*) random ranking and (*upper bound, right*) full dataset training on Flickr30K and COCO.

# pairs	task	R@1			R@5			R@10		
		txt-only	img-only	ours	txt-only	img-only	ours	txt-only	img-only	ours
100	TR	1.3	3.5	9.9	3.5	11.5	28.3	5.9	17.4	39.1
	IR	0.5	1.6	4.7	2.1	5.6	15.7	3.4	9.7	24.6
200	TR	1.4	4.5	10.2	4.8	12.8	28.7	8.2	21.7	41.9
	IR	0.7	2.0	4.6	2.7	8.1	16.0	4.7	13.0	25.5
500	TR	6.6	6.5	13.3	19.5	19.4	32.8	30.4	28.9	46.8
	IR	3.8	3.8	6.6	13.5	12.4	20.2	20.8	19.9	30.0
1000	TR	7.7	5.0	13.3	20.7	17.4	34.8	31.2	24.9	45.7
	IR	4.0	3.9	9.1	13.3	13.1	24.1	20.1	20.1	33.8

Table 4: **Ablation with single modality distillation.** We reported the image-text retrieval performance of text-only distillation, image-only distillation, and our co-distillation on Flickr30K. The results demonstrated the effectiveness of jointly training the model with both text and image.

perform better in a smaller-scale regime (removing spurious information) and text-only distillation to perform better in a larger-scale regime (adding useful details).

In contrast, co-distillation allows the synthetic dataset to optimize further for both compact representation and efficient storage, capable of removing redundant information between examples in the smaller-scale contexts and capable of adding information not present in the selected original images in larger-scale contexts. Our co-distillation method, combining text and image modalities during training, outperforms the single modality distillation approaches consistently across the different number of training pairs and metrics. While the improvement from co-distillation is consistent, it is particularly substantial when the number of pairs is smaller: in the 100 and 200 pairs rows, co-distillation outperforms its unimodal alternatives by over $2\times$. In fact, co-distillation with 100 pairs consistently outperforms unimodal distillation with 1000 pairs. These results demonstrate the effectiveness of jointly distilling across modalities and highlight the complementary nature of multimodal data.

5 Discussion

Conclusion. In this work, we propose a multimodal dataset distillation method for the image-text retrieval task. By co-distilling both the vision and language modalities, we can progressively optimize and distill the most critical information. Our experiments show that co-distilling different modalities via trajectory matching holds promise. We hope that the insights we gathered can be a roadmap for future studies exploring more complex settings, and that our work lays the groundwork for future research aimed at understanding what is the minimum information required for a vision-language model to achieve comparable performance quickly, thereby building a better understanding of the compositionality of compact visual-linguistic knowledge.

Limitations. We note three limitations of our approach. Firstly, dataset distillation is not exempt from the “No Free Lunch” theorem [89]. As discussed in [90], we also observed that the effectiveness of the distilled data is highly influenced by the learning algorithm and model used during the distillation process, which could potentially lead to poor transferability. Secondly, the goal of all dataset distillation work, including ours, is to preserve model performance using only the distilled dataset, but unfortunately it remains quite far out-of-reach for current state-of-the-art. Our multimodal dataset distillation approach outperforms baseline methods with fewer samples, yet it still falls short of full dataset training performance. Lastly, many dataset distillation methods are computationally intensive, i.e. the bi-level optimization in meta-learning distillation approaches, which is another major challenge. In contrast, our trajectory matching approach is significantly less computational demanding, yet we observed that the larger synthetic steps often result in improved performance, and exploring closed-form solutions, i.e. implicit gradient-based methods [17] could be promising future directions to pursue.

Broader Impact. Our exploration is centered on the scientific understanding and practical applications of multimodal dataset distillation. While our work does not directly imply negative impacts, it may indirectly propagate the existing biases in the original datasets. Therefore, it is important to have rigorous bias-mitigation measurements and comprehensive ethical guidelines for dataset distillation. Discussion on these critical aspects should remain a priority as we further explore the potential of multimodal dataset distillation.

6 Acknowledgement

This material is based upon work supported by the National Science Foundation under Grant No. 2107048. Any opinions, findings, and conclusions or recommendations expressed in this material are those of the author(s) and do not necessarily reflect the views of the National Science Foundation. We thank Allison Chen, Tiffany Ling, Jihoon Chung, Carlos E. Jimenez, Ye Zhu, William Yang and Kaiqu Liang for their helpful feedback on this work.

References

- [1] Felipe Petroski Such, Aditya Rawal, Joel Lehman, Kenneth Stanley, and Jeffrey Clune. Generative teaching networks: Accelerating neural architecture search by learning to generate synthetic training data. In *ICML*, 2020.
- [2] Dmitry Medvedev and Alexander D’yakonov. Learning to generate synthetic training data using gradient matching and implicit differentiation. In *AIST*, 2021.

- [3] Felix Wiewel and Bin Yang. Condensed composite memory continual learning. In *IJCNN*, 2021.
- [4] Mattia Sangermano, Antonio Carta, Andrea Cossu, and Davide Bacciu. Sample condensation in online continual learning. In *IJCNN*, 2022.
- [5] Jianyang Gu, Kai Wang, Wei Jiang, and Yang You. Summarizing stream data for memory-restricted online continual learning. *arXiv preprint arXiv:2305.16645*, 2023.
- [6] Ping Liu, Xin Yu, and Joey Tianyi Zhou. Meta knowledge condensation for federated learning. In *ICLR*, 2023.
- [7] Yuanhao Xiong, Ruochen Wang, Minhao Cheng, Felix Yu, and Cho-Jui Hsieh. FedDM: Iterative distribution matching for communication-efficient federated learning. In *CVPR*, 2023.
- [8] Guang Li, Ren Togo, Takahiro Ogawa, and Miki Haseyama. Compressed gastric image generation based on soft-label dataset distillation for medical data sharing. *Computer Methods and Programs in Biomedicine*, 2022.
- [9] Rui Song, Dai Liu, Dave Zhenyu Chen, Andreas Festag, Carsten Trinitis, Martin Schulz, and Alois Knoll. Federated learning via decentralized dataset distillation in resource-constrained edge environments. *arXiv preprint arXiv:2208.11311*, 2022.
- [10] Tongzhou Wang, Jun-Yan Zhu, Antonio Torralba, and Alexei A Efros. Dataset distillation. *arXiv preprint arXiv:1811.10959*, 2018.
- [11] Bo Zhao and Hakan Bilen. Dataset condensation with gradient matching. In *ICLR*, 2021.
- [12] George Cazenavette, Tongzhou Wang, Antonio Torralba, Alexei A. Efros, and Jun-Yan Zhu. Dataset distillation by matching training trajectories. In *CVPR*, 2022.
- [13] Zixuan Jiang, Jiaqi Gu, Mingjie Liu, and David Z Pan. Delving into effective gradient matching for dataset condensation. *arXiv preprint arXiv:2208.00311*, 2022.
- [14] Jiawei Du, Yidi Jiang, Vincent T. F. Tan, Joey Tianyi Zhou, and Haizhou Li. Minimizing the accumulated trajectory error to improve dataset distillation. In *CVPR*, 2023.
- [15] Kai Wang, Bo Zhao, Xiangyu Peng, Zheng Zhu, Shuo Yang, Shuo Wang, Guan Huang, Hakan Bilen, Xinchao Wang, and Yang You. CAFE: Learning to condense dataset by aligning features. In *CVPR*, 2022.
- [16] Bo Zhao and Hakan Bilen. Dataset condensation with distribution matching. In *WACV*, 2023.
- [17] Jonathan Lorraine, Paul Vicol, and David Duvenaud. Optimizing millions of hyperparameters by implicit differentiation. In *AISTATS*, 2020.
- [18] Timothy Nguyen, Zhourong Chen, and Jaehoon Lee. Dataset meta-learning from kernel ridge-regression. In *ICLR*, 2020.
- [19] Timothy Nguyen, Roman Novak, Lechao Xiao, and Jaehoon Lee. Dataset distillation with infinitely wide convolutional networks. In *NeurIPS*, 2021.
- [20] Paul Vicol, Jonathan P Lorraine, Fabian Pedregosa, David Duvenaud, and Roger B Grosse. On implicit bias in overparameterized bilevel optimization. In *ICML*, 2022.
- [21] Noel Loo, Ramin Hasani, Alexander Amini, and Daniela Rus. Efficient dataset distillation using random feature approximation. In *NeurIPS*, 2022.
- [22] Noel Loo, Ramin Hasani, Mathias Lechner, and Daniela Rus. Dataset distillation with convexified implicit gradients. *arXiv preprint arXiv:2302.06755*, 2023.
- [23] Jang-Hyun Kim, Jinuk Kim, Seong Joon Oh, Sangdoo Yun, Hwanjun Song, Joonhyun Jeong, Jung-Woo Ha, and Hyun Oh Song. Dataset condensation via efficient synthetic-data parameterization. In *ICML*, 2022.
- [24] Zhiwei Deng and Olga Russakovsky. Remember the past: Distilling datasets into addressable memories for neural networks. In *NeurIPS*, 2022.
- [25] Balhae Kim, Jungwon Choi, Seanie Lee, Yoonho Lee, Jung-Woo Ha, and Juho Lee. On divergence measures for bayesian pseudocoresets. In *NeurIPS*, 2022.

- [26] Bo Zhao and Hakan Bilen. Synthesizing informative training samples with gan. In *NeurIPS, Workshop*, 2022.
- [27] Ilya Sucholutsky and Matthias Schonlau. Soft-label dataset distillation and text dataset distillation. In *IJCNN*. IEEE, 2021.
- [28] Ce Zhou, Qian Li, Chen Li, Jun Yu, Yixin Liu, Guangjing Wang, Kai Zhang, Cheng Ji, Qiben Yan, Lifang He, et al. A comprehensive survey on pretrained foundation models: A history from bert to chatgpt. *arXiv preprint arXiv:2302.09419*, 2023.
- [29] Rishi Bommasani, Drew A Hudson, Ehsan Adeli, Russ Altman, Simran Arora, Sydney von Arx, Michael S Bernstein, Jeannette Bohg, Antoine Bosselut, Emma Brunskill, et al. On the opportunities and risks of foundation models. *arXiv preprint arXiv:2108.07258*, 2021.
- [30] Alec Radford, Jong Wook Kim, Chris Hallacy, Aditya Ramesh, Gabriel Goh, Sandhini Agarwal, Girish Sastry, Amanda Askell, Pamela Mishkin, Jack Clark, et al. Learning transferable visual models from natural language supervision. In *ICML*, 2021.
- [31] Jacob Devlin, Ming-Wei Chang, Kenton Lee, and Kristina Toutanova. Bert: Pre-training of deep bidirectional transformers for language understanding. *arXiv preprint arXiv:1810.04805*, 2018.
- [32] Yen-Chun Chen, Linjie Li, Licheng Yu, Ahmed El Kholy, Faisal Ahmed, Zhe Gan, Yu Cheng, and Jingjing Liu. Uniter: Universal image-text representation learning. In *ECCV*, 2020.
- [33] Amanpreet Singh, Ronghang Hu, Vedanuj Goswami, Guillaume Couairon, Wojciech Galuba, Marcus Rohrbach, and Douwe Kiela. Flava: A foundational language and vision alignment model. In *CVPR*, 2022.
- [34] Junnan Li, Dongxu Li, Caiming Xiong, and Steven Hoi. Blip: Bootstrapping language-image pre-training for unified vision-language understanding and generation. In *ICML*, 2022.
- [35] Junnan Li, Dongxu Li, Silvio Savarese, and Steven Hoi. Blip-2: Bootstrapping language-image pre-training with frozen image encoders and large language models. *arXiv preprint arXiv:2301.12597*, 2023.
- [36] Scott Reed, Konrad Zolna, Emilio Parisotto, Sergio Gomez Colmenarejo, Alexander Novikov, Gabriel Barth-Maron, Mai Gimenez, Yury Sulsky, Jackie Kay, Jost Tobias Springenberg, et al. A generalist agent. *arXiv preprint arXiv:2205.06175*, 2022.
- [37] Jean-Baptiste Alayrac, Jeff Donahue, Pauline Luc, Antoine Miech, Iain Barr, Yana Hasson, Karel Lenc, Arthur Mensch, Katherine Millican, Malcolm Reynolds, et al. Flamingo: a visual language model for few-shot learning. *NeurIPS*, 2022.
- [38] Aakanksha Chowdhery, Sharan Narang, Jacob Devlin, Maarten Bosma, Gaurav Mishra, Adam Roberts, Paul Barham, Hyung Won Chung, Charles Sutton, Sebastian Gehrmann, et al. Palm: Scaling language modeling with pathways. *arXiv preprint arXiv:2204.02311*, 2022.
- [39] Yann LeCun, Léon Bottou, Yoshua Bengio, and Patrick Haffner. Gradient-based learning applied to document recognition. *Proceedings of the IEEE*, 1998.
- [40] Alex Krizhevsky, Geoffrey Hinton, et al. Learning multiple layers of features from tiny images. 2009.
- [41] Max Welling. Herding dynamical weights to learn. In *ICML*, 2009.
- [42] Mariya Toneva, Alessandro Sordoni, Remi Tachet des Combes, Adam Trischler, Yoshua Bengio, and Geoffrey J Gordon. An empirical study of example forgetting during deep neural network learning. *arXiv preprint arXiv:1812.05159*, 2018.
- [43] Reza Zanjirani Farahani and Masoud Hekmatfar. *Facility location: concepts, models, algorithms and case studies*. Springer Science & Business Media, 2009.
- [44] Ozan Sener and Silvio Savarese. Active learning for convolutional neural networks: A core-set approach. *arXiv preprint arXiv:1708.00489*, 2017.
- [45] Bryan A Plummer, Liwei Wang, Chris M Cervantes, Juan C Caicedo, Julia Hockenmaier, and Svetlana Lazebnik. Flickr30k entities: Collecting region-to-phrase correspondences for richer image-to-sentence models. In *ICCV*, 2015.
- [46] Tsung-Yi Lin, Michael Maire, Serge Belongie, James Hays, Pietro Perona, Deva Ramanan, Piotr Dollár, and C Lawrence Zitnick. Microsoft coco: Common objects in context. In *ECCV*, 2014.

- [47] Yongchao Zhou, Ehsan Nezhadarya, and Jimmy Ba. Dataset distillation using neural feature regression. In *NeurIPS*, 2022.
- [48] Bo Zhao and Hakan Bilen. Dataset condensation with differentiable siamese augmentation. In *ICML*, 2021.
- [49] Bo Zhao, Konda Reddy Mopuri, and Hakan Bilen. Dataset condensation with gradient matching. *arXiv preprint arXiv:2006.05929*, 2020.
- [50] Saehyung Lee, Sanghyuk Chun, Sangwon Jung, Sangdoo Yun, and Sungroh Yoon. Dataset condensation with contrastive signals. In *ICML*, 2022.
- [51] Ondrej Bohdal, Yongxin Yang, and Timothy Hospedales. Flexible dataset distillation: Learn labels instead of images. *arXiv preprint arXiv:2006.08572*, 2020.
- [52] Yongqi Li and Wenjie Li. Data distillation for text classification. *arXiv preprint arXiv:2104.08448*, 2021.
- [53] Justin Cui, Ruochen Wang, Si Si, and Cho-Jui Hsieh. Scaling up dataset distillation to imagenet-1k with constant memory. *arXiv preprint arXiv:2211.10586*, 2022.
- [54] Filip Radenovic, Abhimanyu Dubey, Abhishek Kadian, Todor Mihaylov, Simon Vandenhende, Yash Patel, Yi Wen, Vignesh Ramanathan, and Dhruv Mahajan. Filtering, distillation, and hard negatives for vision-language pre-training. In *CVPR*, 2023.
- [55] Francisco Rivera Valverde, Juana Valeria Hurtado, and Abhinav Valada. There is more than meets the eye: Self-supervised multi-object detection and tracking with sound by distilling multimodal knowledge. In *CVPR*, 2021.
- [56] Ye Zhu, Yu Wu, Nicu Sebe, and Yan Yan. Vision+ x: A survey on multimodal learning in the light of data. *arXiv preprint arXiv:2210.02884*, 2022.
- [57] Ashwini Pokle, Jinjin Tian, Yuchen Li, and Andrej Risteski. Contrasting the landscape of contrastive and non-contrastive learning. 2022.
- [58] Paul Pu Liang, Amir Zadeh, and Louis-Philippe Morency. Foundations and recent trends in multimodal machine learning: Principles, challenges, and open questions. *arXiv preprint arXiv:2209.03430*, 2022.
- [59] Jiacheng Chen, Hexiang Hu, Hao Wu, Yuning Jiang, and Changhu Wang. Learning the best pooling strategy for visual semantic embedding. In *CVPR*, 2021.
- [60] Zhenyu Huang, Guocheng Niu, Xiao Liu, Wenbiao Ding, Xinyan Xiao, Hua Wu, and Xi Peng. Learning with noisy correspondence for cross-modal matching. *NeurIPS*, 2021.
- [61] Sanghyuk Chun, Seong Joon Oh, Rafael Sampaio De Rezende, Yannis Kalantidis, and Diane Larlus. Probabilistic embeddings for cross-modal retrieval. In *CVPR*, 2021.
- [62] Xindi Wu, KwunFung Lau, Francesco Ferroni, Aljoša Ošep, and Deva Ramanan. Pix2map: Cross-modal retrieval for inferring street maps from images. In *CVPR*, 2023.
- [63] Yu-Jhe Li and Kris Kitani. 3d-clfusion: Fast text-to-3d rendering with contrastive latent diffusion. *arXiv preprint arXiv:2303.11938*, 2023.
- [64] Tianlang Chen, Jiajun Deng, and Jiebo Luo. Adaptive offline quintuplet loss for image-text matching. In *ECCV*, 2020.
- [65] Haoran Wang, Ying Zhang, Zhong Ji, Yanwei Pang, and Lin Ma. Consensus-aware visual-semantic embedding for image-text matching. In *ECCV*, 2020.
- [66] Hao Wu, Jiayuan Mao, Yufeng Zhang, Yuning Jiang, Lei Li, Weiwei Sun, and Wei-Ying Ma. Unified visual-semantic embeddings: Bridging vision and language with structured meaning representations. In *CVPR*, 2019.
- [67] Jonatas Wehrmann, Douglas M Souza, Mauricio A Lopes, and Rodrigo C Barros. Language-agnostic visual-semantic embeddings. In *ICCV*, 2019.
- [68] Yale Song and Mohammad Soleymani. Polysemous visual-semantic embedding for cross-modal retrieval. In *CVPR*, 2019.
- [69] Yan Huang, Qi Wu, Chunfeng Song, and Liang Wang. Learning semantic concepts and order for image and sentence matching. In *CVPR*, 2018.

- [70] Jiuxiang Gu, Jianfei Cai, Shafiq R Joty, Li Niu, and Gang Wang. Look, imagine and match: Improving textual-visual cross-modal retrieval with generative models. In *CVPR*, 2018.
- [71] Peter Young, Alice Lai, Micah Hodosh, and Julia Hockenmaier. From image descriptions to visual denotations: New similarity metrics for semantic inference over event descriptions. *Transactions of the Association for Computational Linguistics*, 2014.
- [72] Fartash Faghri, David J Fleet, Jamie Ryan Kiros, and Sanja Fidler. Vse++: Improving visual-semantic embeddings with hard negatives. *arXiv preprint arXiv:1707.05612*, 2017.
- [73] Haiwen Diao, Ying Zhang, Lin Ma, and Huchuan Lu. Similarity reasoning and filtration for image-text matching. In *AAAI*, 2021.
- [74] Kuang-Huei Lee, Xi Chen, Gang Hua, Houdong Hu, and Xiaodong He. Stacked cross attention for image-text matching. In *ECCV*, 2018.
- [75] Zhiqiu Lin, Samuel Yu, Zhiyi Kuang, Deepak Pathak, and Deva Ramanan. Multimodality helps unimodality: Cross-modal few-shot learning with multimodal models. *arXiv preprint arXiv:2301.06267*, 2023.
- [76] Rohan Pandey, Rulin Shao, Paul Pu Liang, Ruslan Salakhutdinov, and Louis-Philippe Morency. Cross-modal attention congruence regularization for vision-language relation alignment. *ACL*, 2022.
- [77] Zhiqiu Lin, Xinyue Chen, Deepak Pathak, Pengchuan Zhang, and Deva Ramanan. Visualgptscore: Visio-linguistic reasoning with multimodal generative pre-training scores. *arXiv preprint arXiv:2306.01879*, 2023.
- [78] Hui Chen, Guiguang Ding, Xudong Liu, Zijia Lin, Ji Liu, and Jungong Han. Imram: Iterative matching with recurrent attention memory for cross-modal image-text retrieval. In *Proceedings of the IEEE/CVF conference on computer vision and pattern recognition*, pages 12655–12663, 2020.
- [79] Aaron van den Oord, Yazhe Li, and Oriol Vinyals. Representation learning with contrastive predictive coding. *arXiv preprint arXiv:1807.03748*, 2018.
- [80] Andrej Karpathy and Li Fei-Fei. Deep visual-semantic alignments for generating image descriptions. In *CVPR*, 2015.
- [81] Olga Russakovsky, Jia Deng, Hao Su, Jonathan Krause, Sanjeev Satheesh, Sean Ma, Zhiheng Huang, Andrej Karpathy, Aditya Khosla, Michael Bernstein, Alexander C. Berg, and Li Fei-Fei. ImageNet Large Scale Visual Recognition Challenge. *IJCV*, 2015.
- [82] Jia Deng, Wei Dong, Richard Socher, Li-Jia Li, Kai Li, and Li Fei-Fei. Imagenet: A large-scale hierarchical image database. In *2009 IEEE conference on computer vision and pattern recognition*. Ieee, 2009.
- [83] Andy Brock, Soham De, Samuel L Smith, and Karen Simonyan. High-performance large-scale image recognition without normalization. In *ICML*, 2021.
- [84] Ross Wightman. Pytorch image models. <https://github.com/rwightman/pytorch-image-models>, 2019.
- [85] Yukun Zhu, Ryan Kiros, Rich Zemel, Ruslan Salakhutdinov, Raquel Urtasun, Antonio Torralba, and Sanja Fidler. Aligning books and movies: Towards story-like visual explanations by watching movies and reading books. In *ICCV*, 2015.
- [86] Kaiming He, Xiangyu Zhang, Shaoqing Ren, and Jian Sun. Delving deep into rectifiers: Surpassing human-level performance on imagenet classification. In *ICCV*, 2015.
- [87] Adam Paszke, Sam Gross, Francisco Massa, Adam Lerer, James Bradbury, Gregory Chanan, Trevor Killeen, Zeming Lin, Natalia Gimelshein, Luca Antiga, et al. Pytorch: An imperative style, high-performance deep learning library. *NeurIPS*, 2019.
- [88] Ryan Kiros, Ruslan Salakhutdinov, and Richard S Zemel. Unifying visual-semantic embeddings with multimodal neural language models. *arXiv preprint arXiv:1411.2539*, 2014.
- [89] David H Wolpert and William G Macready. No free lunch theorems for optimization. *IEEE transactions on evolutionary computation*, 1997.
- [90] Noveen Sachdeva and Julian McAuley. Data distillation: A survey. *arXiv preprint arXiv:2301.04272*, 2023.

- [91] Alexey Dosovitskiy, Lucas Beyer, Alexander Kolesnikov, Dirk Weissenborn, Xiaohua Zhai, Thomas Unterthiner, Mostafa Dehghani, Matthias Minderer, Georg Heigold, Sylvain Gelly, et al. An image is worth 16x16 words: Transformers for image recognition at scale. *arXiv preprint arXiv:2010.11929*, 2020.
- [92] Andrew Brock, Soham De, and Samuel L Smith. Characterizing signal propagation to close the performance gap in unnormalized resnets. *arXiv preprint arXiv:2101.08692*, 2021.
- [93] Jing Xu, Yu Pan, Xinglin Pan, Steven Hoi, Zhang Yi, and Zenglin Xu. Regnet: self-regulated network for image classification. *IEEE Transactions on Neural Networks and Learning Systems*, 2022.
- [94] Kaiming He, Xiangyu Zhang, Shaoqing Ren, and Jian Sun. Deep residual learning for image recognition. In *Proceedings of the IEEE conference on computer vision and pattern recognition*, pages 770–778, 2016.

Appendix

In this Appendix, we further extended the ablation study, analyzing components of our pipeline, i.e. distilled dataset initialization (Sec. 7.1), encoder backbones (Sec. 7.2), pretraining (Sec. 7.3), synthetic steps (Sec. 7.4). We also include additional visualizations of the distilled samples (Sec. 8) for both Flickr30K and COCO.

7 Additional Ablation Studies

In this section, we provide additional ablation studies. Unless specified, these distillation experiments are conducted on the Flickr30K dataset to distill 100 image-text pairs, and we use pretrained NFNet and BERT as backbones, with synthetic step set to 8 during distillation.

7.1 Distilled Dataset Initialization

In the main paper, we provided experiments with real sample initialization. Here we experiment and evaluate initializing with Gaussian noise. Our findings in Tab. 5 show that initializing images from Gaussian distribution results in significantly lower performance. It is worth noting that the complexity of images, encoding a high degree and rich information of colors, shapes, textures and spatial relationships between objects, can make it difficult for models to learn effectively from randomly initialized images. On the other hand, using real text sampled from the training set vs. randomly initialized text embeddings does not have a significant difference. Our assumption is, the pretrained language models are good at generating or transforming ‘noise’ text embedding into meaningful sentences during the learning process, partly due to the inherent structure and predictability of language. We provide visualizations of the combination of real image and ‘noise’ text below in Fig. 4 and Fig. 5 and Tab. 7.1. To our surprise, even though the initialized ‘noise’ texts are not semantically meaningful to the initialized real images, we discovered a substantial degree of semantic similarity between the initialized real images and the learned distilled text. This suggests the probability of future application of our method in Visual Question Answering (VQA).

Real Image	Real Text	Distillation					
		TR			IR		
		R@1	R@5	R@10	R@1	R@5	R@10
✓	✓	9.9	28.3	39.1	4.7	15.7	24.6
✓		9	27.2	40.1	3.9	13.2	20.6
	✓	0.2	0.7	1.1	0.1	0.5	1
		0.1	0.3	0.4	0.1	0.4	0.8

Table 5: **Image-Text Pair Initialization.** We compare the retrieval performance achieved with different combinations of image and text initialization strategies. The ✓ denotes the use of the real image or text directly sampled from the training set, otherwise indicates the use of randomly initialized image or text, following Gaussian distribution. We can see that if we initialize the image from scratch, the performance will be pretty low. On the contrary, the performance did not drop too much if we start with ‘noise’ texts and real images, which indicates the importance of image signal for the small distilled set.

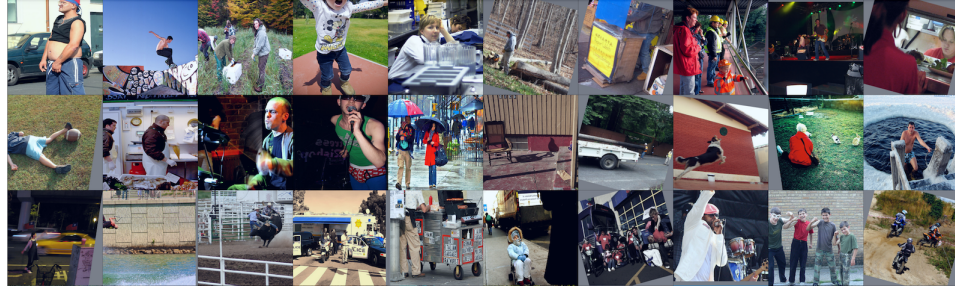


Figure 4: Real Images, iteration = 0

‘noise’ Texts, iteration = 0. 30 randomly initialized text from Gaussian distribution, we use nearest neighbor to find their closest sentence in the training set in Flickr30k for visualization purposes.

this man is fit and well toned running enthusiast
the music concert is just started at the giant stadium
a man in a beige shirt and tan slacks sits in a chair next to a hospital patient wearing a
blue gown who is sitting cross-legged on his hospital bed
man and woman employed by mongolian barbecue stand at counter
woman cupping water with hands over bathroom sink as child stands beside her
near snowflake sign, man sits while another stands wearing badge and headphones
very brave snow skier doing a flip off a cliff
a guy, dressed nicely, is painting a mural on a wall, with a ladder sitting beside him
dog chasing brown cow and black cow
seems to me looks like people in a work room or office working they all using laptop computers
from apple it seems there dr pepper soda and water bottle on
olympian performing on the rings
man walking behind distracted-looking woman carrying bags and camera
three men in caps sit at fireside near cabin, reading at night
the dog with the red collar is white, black, and brown
minor league pitcher
man in chair laughing and talking to others, while handling books
the man, with no shirt, reaches into a bucket to extract the substance inside small brown dog
on leash
woman sitting at a park bench reading a book
violin soloists take the stage during the orchestra’s opening show at the theater
black dog sitting while eating with neon yellow band around shoulders
several people are standing under a tarp two ladies are facing each other and one has a
backpack on with her hands in her jeans pockets while the other one
a boy wearing a flowered shirt raises his arm and jumps
a quarterback is looking to set up a pass from the end zone, while a teammate provides some
blocking
a woman in a red coat takes a picture near marble columns at twilight
people with anti-immigration signs
the outside of a restaurant called el triuneo
cheerleaders build a pyramid near the goal-line
baby wears green frog big and makes grotesque face
a yellow, suspended roller coaster on a yellow track is midway through a loop

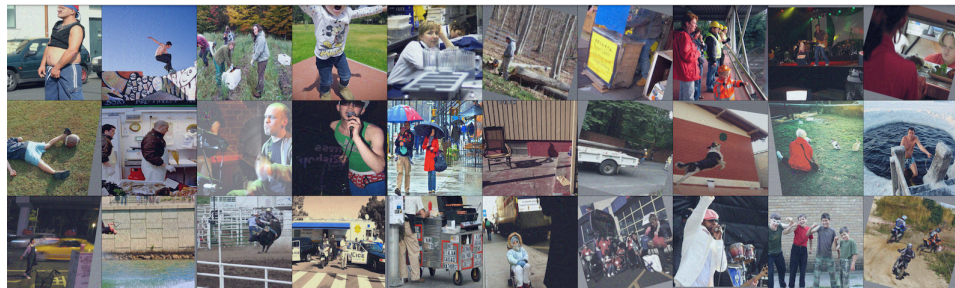


Figure 5: Distilled Images, iteration = 1000

Distilled Texts, iteration = 1000. Starting with randomly initialized text from Gaussian distribution, here is the synthetic text after distillation.

superhero man leaping in a plaza
a guy in a blue shirt listens to music as he skateboards along the edge of a ramp
tiger woods about to make a putt
little boy pulling a green wagon wearing a sweatshirt and boots
a young girl with blond-hair and glasses sitting at a table in a restaurant
three black young man are working in a semi-deserted area with a pile of construction material
and jugs, one of them is digging
woman buying cups of fruit from street vendor
six men in blue jumpsuits and a man in an orange jumpsuit walk by a shipyard
young girl balances on a reclined man's legs as part of a performance in front of an audience
a woman fillets a fish, as part of preparing a recipe that includes broccoli, celery, and eggs
a young man wearing a white shirt and red shorts kicking a ball
contortionist in strange checkered outfit wearing a white mask
one man plays an acoustic guitar, while another accompanies him on the accordion
male wearing brown shirt holding a microphone with an expression of singing
a young lady in a colorful dress, holds a white stuffed animal stands in the rain hold a plaid
umbrella
a person with blue and polka-dot socks jumps on a bed with a red and white blanket
a damaged black color car on the street
skateboarder jumping in air and his skateboard is between his legs
a woman with a guitar sings in front of a building and grass
two woman are sitting on a beach together, facing the water
a busy street with building lined up and people walking down the street outside and nighttime
parasailer doing flip in midair
crowded arena with lots of people wearing yellow, carrying red flags
men in turbans laying down and examining cloth
a woman in a white apron prepares various meats on a large grill
a middle-aged man in a trench coat sleeps on a bus or train
a line of people, some standing and some sitting, are waiting on a platform for a train
three men playing drums, bass, and piano
a dirt-blond girl in a white top with a key necklace holds a bag, standing in front of a
sidewalk of street
cattle-drawn wagons traveling down a paved road and loaded with sticks

7.2 Encoder Backbone Selection

This section delves into the selection of vision and language backbones. We introduce the **Performance Recovery Ratio (PRR)** to evaluate the effectiveness of dataset distillation. It quantifies the percentage of performance retained from the original data. The performance for various backbone combinations is shown in Table 8.

7.2.1 Language Backbones

Perhaps not surprisingly, CLIP [30] text encoder significantly outperforms BERT in all evaluation metrics, with a striking peak performance in TR R@10 at 92.8% for expert training. This exceptional performance can be mainly attributed to the fact that the pre-trained, off-the-shelf CLIP model is designed to learn a shared embedding space across multi-modalities. Although CLIP also shows a performance drop during distillation, it still retains a relatively high performance recovery ratio. In Sec. 8 we provide visualization of synthetic data distilled via NFNet and CLIP in Tab. 8 and Fig. 10, Fig. 11.

Language Model	Expert						Distillation					
	TR			IR			TR			IR		
	R@1	R@5	R@10	R@1	R@5	R@10	R@1	R@5	R@10	R@1	R@5	R@10
BERT	33.9	65.1	75.2	27.3	57.2	69.7	9.9	28.3	39.1	4.7	15.7	24.6
CLIP	61.2	87.5	92.8	49.8	79.8	88.3	31.4	58.8	72.0	17.1	41.9	56.2

Table 6: **Ablation Analysis on Language Backbones.** We provide expert training and distillation performance evaluation for both pretrained BERT and CLIP models. CLIP text encoder demonstrates a strong capacity for high-recall retrieval.

7.2.2 Vision Backbones

The vision encoders carry the main gradient flows for the distillation process. We experimented on several vision backbones, and found that the architecture choice strongly influences the distillation quality. Similar to dataset distillation by gradient matching [11], batch normalization has an impact on the gradient/parameter matching framework. This is mainly because batch normalization

incorporates a non-parametric component that can only be accumulated with batches and can not be trained. Interestingly, the Vision Transformer (ViT) [91] also struggles to perform well in distillation, potentially due to attention mechanism. We leave this for further studies.

Vision Model	Expert						Distillation					
	TR			IR			TR			IR		
	R@1	R@5	R@10	R@1	R@5	R@10	R@1	R@5	R@10	R@1	R@5	R@10
NFNet-l0	33.9	65.1	75.2	27.32	57.12	69.68	9.9	28.3	39.1	4.7	15.7	24.6
VIT_Tiny	20.4	46.5	59.7	16.64	40.16	53.76	0.3	0.8	1.3	0.1	0.76	1.5
NF_ResNet50	28.9	56.6	71	22.84	50.12	63.42	6.5	18.2	28.1	3.46	11.56	18.66
NF_RegNet	26.9	57.2	70.2	21.08	50.08	62.9	7.8	21.9	33.3	3.28	12.66	20.54
ResNet50	18	43.5	59.5	13.42	36.58	49.96	0.5	2.4	3.8	0.28	1.64	3.62

Table 7: **Ablation Analysis on Vision Backbones.** We provide an extensive evaluation of several pretrained vision backbones including NFNet_l0 [83], VIT_Tiny [91], NF_ResNet50 [92], NF_RegNet [93], and ResNet50 [94] from the timm library [84]. This underscores the influence of architecture and highlights the potential negative impact of batch normalization and attention operations for distillation.

Vision Backbone	Language Backbone	TR			IR		
		R@1	R@5	R@10	R@1	R@5	R@10
NFNet-l0	BERT	29.2%	43.5%	52.0%	17.2%	27.5%	35.2%
VIT_Tiny	BERT	1.5%	1.7%	2.2%	0.6%	1.9%	2.8%
NF_ResNet50	BERT	22.5%	32.1%	39.6%	15.1%	23.0%	29.4%
NF_RegNet	BERT	29.0%	38.3%	47.4%	15.6%	25.3%	32.7%
ResNet50	BERT	2.8%	5.5%	6.4%	2.1%	4.5%	7.2%
NFNet-l0	CLIP	51.31%	67.2%	77.58%	34.36%	52.44%	63.63%

Table 8: **Performance Recovery Ratio (PRR).** The combination of VIT-Tiny and BERT has the lowest PRR. The combination of NFNet-l0 and CLIP demonstrates the highest PRR across all metrics in both TR and IR tasks, with 100 distilled samples, it reaches the impressive PRRs of 51.31% (R@1) in TR, and 34.36% (R@1) in IR on Flickr30K.

7.3 Pretrained vs. Non-pretrained

Table 9 demonstrates the influence of pretraining of the backbone encoders. Optimal performance is observed when both language and vision backbones are pretrained. This emphasizes the importance of pretraining before the expert training phase for large models and datasets.

Language Backbone	Vision Backbone	Expert					
		TR			IR		
		R@1	R@5	R@10	R@1	R@5	R@10
✓	✓	33.9	65.1	75.2	27.32	57.12	69.68
✓		4.4	14.1	20.7	3.5	11.4	18.76
	✓	0.5	1.1	1.8	0.26	0.7	1.42
		0.3	1	1.5	0.14	0.68	1.28

Table 9: **Pretraining Impact.** Expert performance comparison for different pretraining configurations of vision and language backbones. The checkmark (✓) indicates the model was pretrained.

7.4 Synthetic Steps

The synthetic step size plays an important role in optimizing the dataset distillation performance, as shown in Table 10. Using smaller synthetic steps tends to prolong the distillation process, particularly for smaller distilled sets.

#Pairs	#Syn Steps	Distillation					
		TR			IR		
		R@1	R@5	R@10	R@1	R@5	R@10
100	1	0.5	2.1	4.4	0.3	1.5	2.8
	2	7.1	23.4	32.9	3.0	10.2	16.4
	4	8.2	24.9	35.2	3.5	12.2	20.7
	8	9.9	28.3	39.1	4.7	15.7	24.6
200	1	3.2	9.3	14.1	1.6	5.2	8.8
	2	6.5	19.2	29.1	1.6	5.9	10.0
	4	8.2	24.5	34.4	2.2	7.4	11.8
	8	10.2	28.7	41.9	4.6	16.0	25.5
500	1	6.6	18.1	25.5	2.1	10.1	16.3
	2	8	21.7	31.3	3.8	14.9	23.2
	4	8.1	23.6	34.9	4.4	15.2	23.7
	8	13.3	32.8	46.8	6.6	20.2	30.0
1000	1	7.3	20.6	29.7	3.9	13.2	20.7
	2	8.8	26.8	36.6	5.7	17.4	26.4
	4	10.4	29.1	37.9	6.6	19.5	29.5
	8	13.3	34.8	45.7	9.1	24.1	33.8

Table 10: **Synthetic Steps Impact.** Larger synthetic steps greatly improve performance. For 100 pairs with a synthetic step of 1, the performance is even below random selection. Setting the synthetic steps to a low value typically takes longer to optimize the distilled set and it is challenging with very small sets (e.g., # Pairs=100).

8 Additional Visualizations

Here we include a number of visualizations of the data we distilled from the multimodal dataset (both Flickr30K Tab. 8 and Fig. 6, 7 and COCO Tab. 8 and Fig. 8, 9) for a more intuitive understanding of the distilled set. We provide 50 distilled image-text paired examples including their visualization before the distillation process. Unless otherwise stated, these experiments are conducted using 100 distilled pairs, with pretrained NFNet [83] and BERT [31] as backbones and the synthetic step is set to 8 during distillation. We provide visualization of distilled data using NFNet and CLIP in Tab. 8 and Fig. 10, 11 in the end.

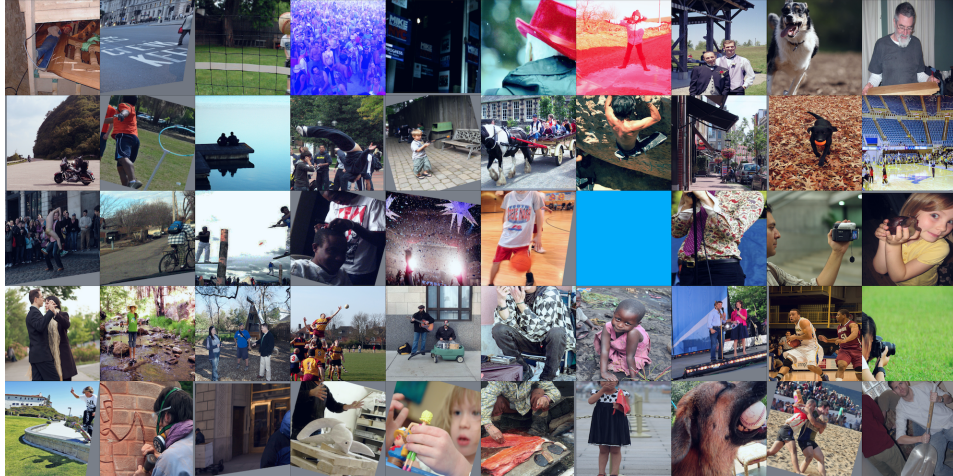


Figure 6: Flickr30K Image Initialization, iteration = 0.

Flickr30k Text Initialization, iteration = 0.

a construction worker stares down a flight of stairs being built
a man in a suit walking across a city street
a child hits a baseball into a net
a large crowd of people
an old man, behind him on glass is many political advertisements
an old man with white hair in a red hat
a young girl, on a road, playing on the ice
two men dressed up before a big event
a dog is running through a field with its tongue hanging out
an older man in a gray shirt with a white long-sleeve shirt under it holding up a small wooden cabinet
a motorcycle is parked along side a mountain road while another goes down the road
a man in an orange shirt and black shorts throws a ball through a hoop while another man watches
two people sit on the end of a dock
a man performs a back flip while preparing for an outdoor performance or competition
a little boy plays with a toy gun
a bunch of young children are riding on the back of a trolley while being carried by a black and white horse
a man climbing up on a rock ledge
a young man sits on a bench in a downtown setting
a black dog carries an orange ball, walking on the ground covered in leaves
basketball players practicing for their game
a man in just his underwear jumping on a man surrounded by a crowd of people
a man wearing lots of plaid riding a bike through the streets
men are trying to cut down trees
a black man getting a haircut
this was a big new years event the people were sing and dancing all night
a boy wearing a steve nash shirt dribbles a basketball on an indoor court
a series of men taking a break from riding their motorcycles
a brown-haired man in a patterned shirt and purple tie is singing into a microphone
a curly dark-haired man holds a small camcorder and films in a person in front of him
a young girl in a yellow shirt holds a rather large snail in her hands next to her cheek
two young men dancing in the street
a girl standing in a shallow creek, wearing stilts
3 people standing on a park talking to each other
a group of young men in colorful uniforms playing with a white ball
two guys are on the side of the street playing a guitar and drums
a mime applying his makeup
a child decorates a shoe with colorful sticks
a man and a woman are up on a stage with microphones in their hands
two basketball players on opposing teams, one in white, the other in red, are mid-game, running down the court, white-uniform player with ball-in-hand
one young lady with black hair in a ponytail wearing a black bracelet and a white shirt, taking pictures with a black camera that has a shoulder strap laying in
a boy on a skateboard is on a wall near the water and next to grass
a sculptor is carving a picture of a knight into a brick wall
a man in a blue coat is walking on the sidewalk
an old man wearing glasses is holding a stick
child playing with doll-like toy
an old man wearing a hooded sweatshirt is crouched over a fish that has been cut open
a young girl in a black dress is holding a red flag and covering a happy expression
a brown dog with a baseball in its mouth
man in white and red tackling man in green shirt for the ball
a man in a white t-shirt is holding a snow shovel

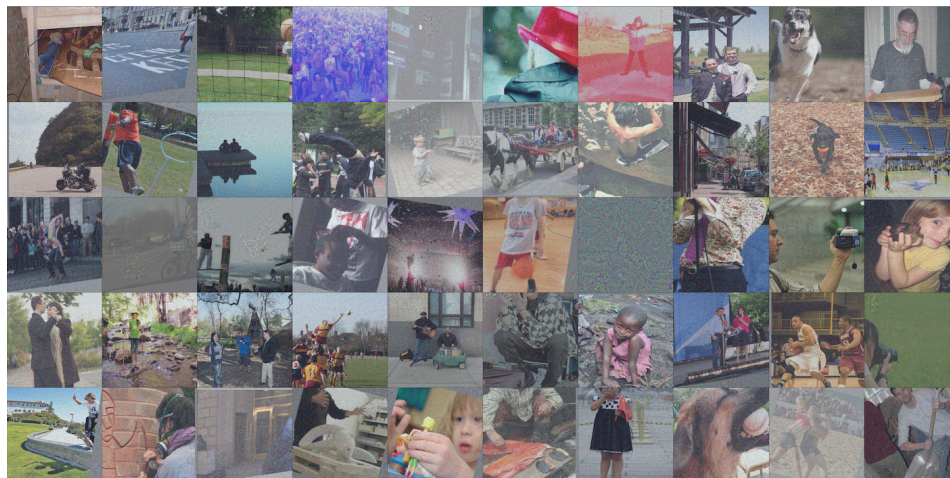


Figure 7: Flickr30K Synthetic Images, iteration = 2000.

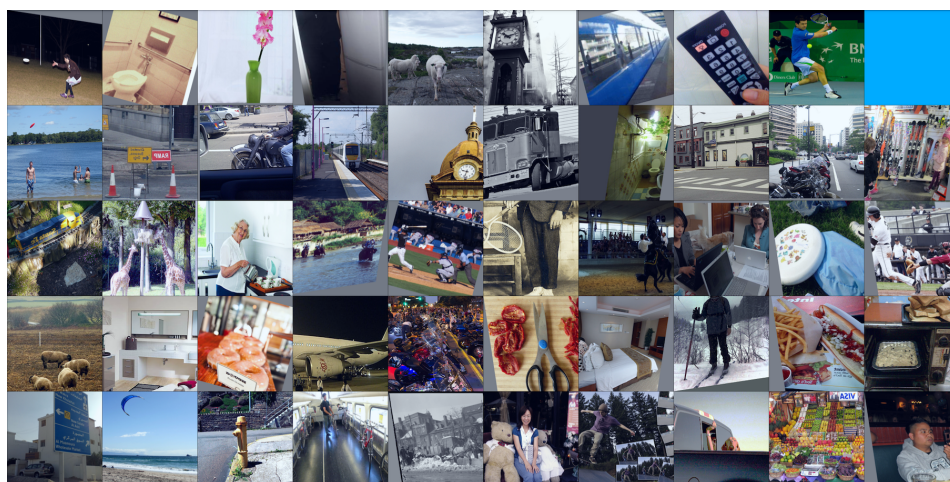


Figure 8: COCO Image Initialization, iteration = 0.



Figure 9: COCO Synthetic Images, iteration = 2000.

Flickr30k Synthetic Texts, iteration = 2000.

construction workers repair walls of a subway
a ship in a harbor at night with a city skyline behind
baseball pitcher throwing a pitch
group of people sitting around a table for a meeting
a man points to something as he is talking to a woman wearing white pants, as they stand in front of a store
man in red sweater with a backwards hat
women wearing winter coats crossing the street next to parked cars and walking down street
the bridal party poses with the bride and groom, all wearing black except for the bride
an old lady, wearing a red hat, is standing on the sidewalk of a park
a man grilling hotdogs and sausages
a motocross bike kicks up dirt as it is being ridden around a bend in the circuit
nine women in blue and purple dresses and one man wearing a purple shirt and black pants, clap while a man dressed in black dances
two young men and two boys are sitting down on a boat next to an anchor and watching the water while playing soccer, a man in yellow starts to fall, while a man in white trips over him, stepping on his ankle in the process
a little boy is walking on a fallen tree in the woods
a jockey and horse in the middle of other jockeys and horses during a race, in the middle of jumping over a hurdle
an extreme man snowboarding up side down a mountain
one man, in a blue jacket, is sitting in the rain under a green umbrella
the brown and white dog is running to catch something
boy takes a bath with diving mask and snorkel
angry looking businessman walking down sidewalk
a person on a bmx bike, leaping onto a bench
two people and a dog are in the snow
young shirtless boy sleeping on a couch with his hand on his chest
a person spins a sparkler around at night and sparks fly through the air and across the ground
a woman, wearing sunglasses, a red athletic top, and running shorts competes in a marathon
a ballet dancer wearing a blue tutu doing the splits, mid-leap
woman on street corner smiles and talks on her cellphone
policeman taping off an area by a group of firemen
a man with a beer and another man facing each other, talking
a woman and two children reading outside on a stone bench
man on motorcycle riding in dry field wearing a helmet and backpack
a man in a white shirt and black exercise shorts walks on a sidewalk, which is located behind a street under construction and in front of a two garage house
a man is hitting a golf ball out of a sand trap, there are green grass all around him
some young adults are playing saxophones and clarinets outdoors
a young man sitting on a rock on the shore of a body of water looking contemplative
a young boy, covered in mud, plays on the beach
shirley manson poses in front of a microphone on stage while holding a large blue, red, and white flag behind her
two hockey players playing offense and defense
a group of friends, 3 boys and 2 girls, jump in the air holding hands for a photo
a boy skateboards and does a jump over another skateboard
ginger baby playing with a train setup made out of counterfeit lego
a group of choreographed rollerskaters dancing
little blond girl in her jacket sticking out her tongue while holding a red balloon
a blond little girl wrapped up in a pink care bears blanket
an oriental man, wearing a white shirt and apron is cooking
one boys sits on a giant mortar gun as another boy walks toward him
brown dog trying to bite a white ball with yellow, green and blue puppy toes
woman standing on the shore of a beach
2 males, one in a red shirt and one in a yellow shirt, cleaning a room

COCO Text Initialization, iteration = 0.

a photo taken at night of a young man playing frisbee
a bathroom toilet is surrounded with silver handrails
a pink flower is sticking out of a green vase
a woman poses next to a fridge
a small group of sheep on the coast
a black and white photo showing a large clock tower on a building
the people are waiting to be picked up
a hand holding a black television remote control
a man swinging a tennis racket at a tennis ball
a man holds a small animal to his face
three people are in the water as a frisbee is in the air
yellow and red street signs warning larger vehicles in a large city
a man riding on the back of a motorcycle
the train is traveling down the railroad tracks
a building with a large clock on it
a man standing on a wheel of a big tarck
a small bathroom with a toilet, sink and window
a florist shop and other buildings on and near a street corner
a line of motorcycles parked on a street
two young girls in a store looking at skis
a small toy model train on a track
a couple of giraffes are outside in the wild
a woman pouring coffee into cups on a counter
people riding on top of elephants across a river
a hitter swings at the baseball and misses
an old picture of a guy holding a tennis racquet
there are people watching three men on horseback
two people sitting at a table with laptops
there are many things laying on the ground
a batter swings hard at a low ball as the catcher reaches out his glove
five sheep stand around a large dirt field
a bathroom with a sink, mirrors and chair
glazed donut sitting on a wooden table top in a donut shop
a huge chinese aircraft is sitting at an airport with people unloading
a bunch of motorcycles are parked together outside
cutting board with scissors and dried food on it
a clean, decorated bedroom is pictured in this image
a man standing on skis at the top of a hill under high tension wires
a long hot dog and french fries are on a plate
a pan of dough is going into the dirty toaster oven
a road sign with both english and arabic directions
a kite being flown on the beach while people watch
a yellow fire hydrant is on the corner of an old sidewalk
a man with a bicycle and a helmet on his head in a subway car
a horse struggles to draw a loaded cart through piles of snow
a woman is sitting between two large teddy bears
a kid skateboarding while other kids stand and watch
there is a dog in the back of the truck
a large assortment of fruits lie on display in a market
he's taking a picture of his friends at the restaurant

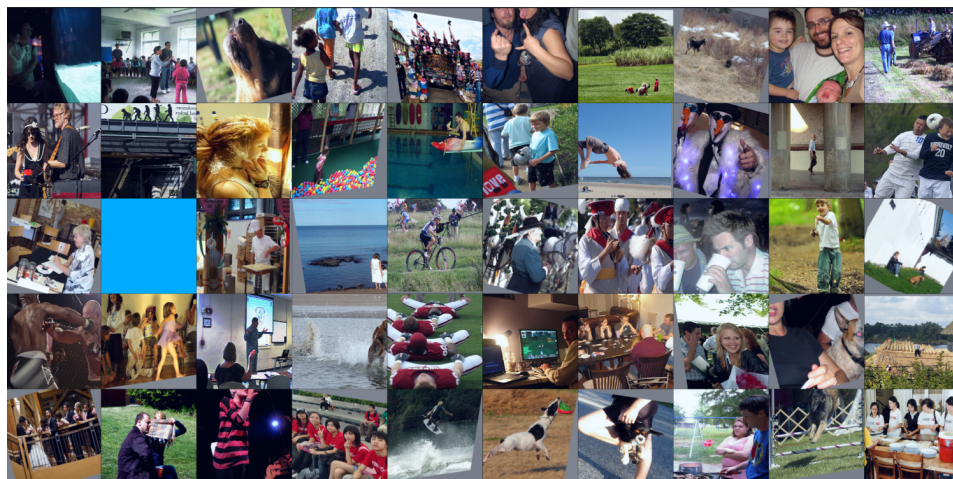


Figure 10: **CLIP**, Flickr30K Image Initialization, iteration = 0.

dog flying in mid-air running after a frisbee
 bath tub with metal shower head, vanity mirror, and small utilities compartment
 a white vase with pink flowers and large green stems
 this apartment has an kitchen with a refrigerator, stove, dishwasher, and cabinets
 a ski resort with many people gathered around the outside lodge
 grandfather clock hanging on wall next to a grandfather clock
 the kitchen is brightly lit from the window
 someone is playing with a nintendo wii controller
 a woman swinging a tennis racket, while standing on a tennis court
 a jet plane taking off into the air
 a sign warning people to stop at red lights
 man swinging baseball bat with ball in air and crowd watching
 a man hitching a trailer with water sports equipment to a sports utility vehicle
 four trains lined up at the train station
 a large tower has a clock towards the top
 people standing at a bus stop about to board a bus
 a small bathroom with a sink a mirror
 man admiring a motorcycle in parking lot, near a large building
 a motorcyclist in a red and white suit riding a red and white motorcycle
 a little boy playing tennis on a tennis court
 a locomotive train resting on some tracks next to a building
 two giraffes graze on some tall plant feeder
 woman looking at camera while lying in bed
 a herd of adult elephants with a baby elephant waling through a forest
 baseball batter in a wide stance, waiting for a pitched ball
 the cars were parked along the street near the traffic light
 the travelers are getting around by horses
 a cluttered desk with a laptop opened to flickr
 the lady is sitting on the wood bench
 a baseball player is preparing to swing a baseball bat
 two lambs eating hay from ground of a field
 some brown cabinets a black oven a tea kettle and a microwave
 the reception ifs full of professional people
 baseball batter ready to strike arriving ball and umpire waiting to catch if he misses
 there lot of motorcycles park in a line with a white car, a red car and a van park not far
 from the motorcycles while there is man riding on
 a very clean room and a pair of scissors
 the bedroom has a wood closet and bookcase near the bed
 a line of skiers heading towards a cabin in the mountains
 a plate topped with onions rings next to a hamburger and hot dog
 the personal sized pizza has been topped with vegetables
 a sign letting people know about the castle rising castle
 girl and two males standing on a beach
 there is a white fire dyrant on the corner street
 a man skateboarding on street in front of a bus
 vintage black and white photograph of two baseball players
 raggedy ann doll sitting in a chair with a pooh bear
 blonde haired boy doing a jump while riding a skate board
 a dog driving a car down a street
 there are bananas, apples and oranges in the bowl,
 a stop light with the green light lit

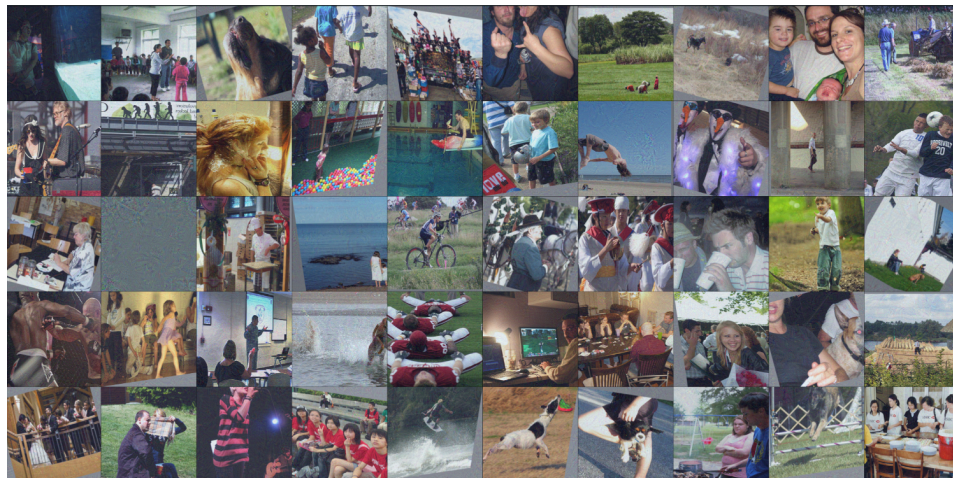


Figure 11: CLIP, Flickr30K Synthetic Images, iteration = 2000.

CLIP, Flickr30k Text Initialization, iteration = 0.

a woman holding a child is standing in front of a tank
a woman and man with a child in the center of a circle of children
a black and brown dog eyeing a fly
four kids next to a blue house are walking down a street
tourists look at merchandise on a street vendors display in england riffling through cards and maps
two people wearing blue clothing are making hand gestures next to one another
four workers in a field harvesting
a dog approaches a small creature in a barren, snowy field
a woman holding a baby and a man in glasses holding a small boy smile at the camera for their family photo
four men are harvesting a crop on a farm
two musicians on stage in front of a microphone stand
a man in a suit is walking under a metal bridge
girl getting her hair dyed
a child is in a ball pit while three adults watch her
a man is sitting in a small kayak on a diving board
a boy in a blue shirt holds a toy helmet in his hands while standing on a path in a park
a boy doing a flip in the air at the beach
two men are dressed up as snowmen
a man walking underneath a bridge glances at the camera
two soccer players are about to butt heads getting the ball
a woman is at an art studio, painting a mural from her art supplies
a boy wearing a black wetsuit stands on a crowded beach
a chef prepares a table with food behind it
two blond girls in white dresses, one much smaller than the other, stand on the bank of a large body of water
a man on a black mountain bike rides through a course filled with other bikers
a man in a hat stands with decorated horses around him
an asian marching band with uniformed members in beige, yellow, and red play in the street
two men with angry faces drink out of white cups
young boy plays with leaves in a green wooded area
a person siting against a wall with a dog
one fighter delivers a hard blow to the face of another fighter
a young group of children sitting in a row against the wall
a teacher stands in front of a projector and a student at the front of the class has her hand raised
a dog is running in a large body of water causing it to splash
football players are stretching together
man playing video game instead of working
a group of people at dining table playing a card game
young woman celebrating her graduation
a dog looks on as a woman eats
a man wearing a flannel shirt and black pants is working on a new reed roof on top of a house
newly married couple having their first kiss
a woman plays hide-and-go-seek with a check scarf as she sits with a man in a dark colored jacket
a woman with short blond-hair smiling and singing into a microphone while a man in a striped shirt, further back, plays an acoustic guitar
a group of asian teenagers wearing red t-shirts sit on steps
a man gets lots of air time as he wakeboards
a black and white dog is running through the field to catch something in its mouth
a person with a small dog caught in her legs
a young man tends chicken wings on a barbecue while a young woman in a pink shirt watches
black and brown dog jumping over hurdle with white supports
a group of women wearing shirts that say, hsbc is standing by a table with food on it

CLIP, Flickr30k Synthetic Texts, iteration = 2000.

a young asian girl petting an animal of some sort and the animal is laying down enjoying it
a group of men in ethnic dress are dancing
brown and tan dog, mouth open with tongue hanging out, running in the grass
an older black woman wearing a colorful print dress stares directly at the camera
woman in red shirt shopping in a outdoor market
a woman in a blue shirt with no bra
a man holding a bag walking down a long staircase
a man in black walking down a street
a woman holds a baby in a blue jumper
a small car in an open field
a group of male musicians are playing instruments including guitar and drums
a man is standing inside a subway train with his mouth wide open
a barber shaving someone's head
a group of people are shopping in what looks to be a christmas store filled with colorful toys
a man in high rubber boots and a plaid shirt is pushing a broom over the mossy blacktop
three males with cameras near each other, two sitting and the third standing, in what might be
a park during a sunny day
a girl jumping up in the air with her hands above her head
two people, one of whom is in a santa costume, pose wearing funny glasses
a group of people walking through an alley along a cobblestone street, between two buildings
a soccer player in a green jersey kicks a blue and yellow ball
a man painting over graffiti
two dogs running near a river while one dogs in swimming in it
a man in a black hat looks surprised at the deli counter
a woman sits in a chair on the beach, backdropped by the ocean
a young man popping a wheelie on his bicycle while riding down a country road
a person attempts to rope a black cow while riding a horse
men dressed in red and white playing musical instruments
two men drink beer out of tall drinking glasses
a little boy is eating on a sidewalk
a man is standing inside a doorway that is in a wall painted with a mural of a woman
a man wearing a hat has his eyes closed, as another man in a red shirt is licking his face
a family of 3 sits and poses on a couch together
a young boy in a sports uniform stands in front of a group of children
a little boy plays outdoors in water spurting up from an inground fountain
two men in red pants do acrobatics with a ladder
a young caucasian man sits at a desk using a laptop computer
a group of people is sharing a meal at a large table at a restaurant
a group of people protest with one holding up a cardboard sign
a group of people and their dogs at a dog show
a man with a plaid shirt is working on some wood in his workshop
the fellow in the black suit at a formal occasion has a salmon rose in his lapel
a man and a woman walking across a field of grass
a woman singer holding a microphone singing at a concert
young asian female sitting in a pose on a stone wall as she is being photographed
the man is standing by a creek in blue flannel shorts
a black and white dog leaps to catch a frisbee in a field
a man is feeding two exotic birds
an asian chef is in the foreground, working over a steaming grill while a younger man is
behind him
a young man is skateboarding down the railing of some stairs
a female chef examines a piece of bread while showing it to the camera
